35th Annual International Conference of the IEEE EMBS
Osaka, Japan, 3 - 7 July, 2013

Design and Analysis of an Antenna for Wireless Energy Harvesting in a Head-mountable DBS Device

Md Kamal Hosain, Abbas Z. Kouzani, Susannah J. Tye, Osama A. Abulseoud, and Michael Berk

Abstract—**This paper presents design and simulation of a circular meander dipole antenna at the industrial, scientific, and medical band of 915 MHz for energy scavenging in a passive head-mountable deep brain stimulation device. The interaction of the proposed antenna with a rat body is modeled and discussed. In the antenna, the radiating layer is meandered, and a FR-4 substrate is used to limit the radius and height of the antenna to 14 mm and 1.60 mm, respectively. The resonance frequency of the designed antenna is 915 MHz and the bandwidth of 15 MHz at a return loss of -10 dB in free space. To model the interaction of the antenna with a rat body, two aspects including functional and biological are considered. The functional aspect includes input impedance, resonance frequency, gain pattern, radiation efficiency of the antenna, and the biological aspect involves electric field distribution, and SAR value. A complete rat model is used in the finite difference time domain based EM simulation software XFdtd. The simulated results demonstrate that the specific absorption rate distributions occur within the skull in the rat model, and their values are higher than the standard regulated values for the antenna receiving power of 1W.**

I. Introduction

Finite battery life time, battery size, and battery replacement difficulty in head-mountable Deep Brain Stimulation (DBS) devices, plus some generic environmental concerns associated with the use of batteries [1] are encouraging researchers to develop battery-less DBS devices. For miniature, low power consumption devices, the battery can be replaced by an energy harvester that captures energy from ambient sources [2]. Currently, the energy harvesters are used in passive RFID tags [3]. Harb [4] presented a good description of the energy harvesting approaches.

An energy harvester captures energy from the ambient sources that exist around a device. The sources include thermal, solar, vibration, electromagnetic wave, acoustic, etc. [1, 4, 5, 6]. Up to date, the energy harvested from ambient sources is within the range of a few mW. The development of new ultra-low power electronic devices is currently steering the energy harvesting research. At present, the power consumption rate of the available discrete circuit components typically is: sensors 120μA, microcontrollers 160μA/MHz, transceivers (RS-485) 120μA [1]. Whilst the energy scavenging from ambient sources is an attractive solution in low power consumer electronics, it is difficult to get sufficient energy for an implant from the sources around us [7]. In addition, by considering safety and reliability, the head-mountable DBS device is considered which can get energy from a far field source of collimated beam of transmitted radio frequency (RF).

The main part of a wireless power scavenging device is a rectenna which consists of an antenna and a rectifying circuit. The antenna receives the far field collimated RF EM wave as a source of energy. The rectifier circuit converts the energy received through the antenna to DC power which is then used to operate the DBS device.

In DBS research with animals especially rats, a head-mountable device can be used. A passive head-mountable DBS device comprises an antenna on board of the device for receiving far field power. When an antenna is mounted on the head of a rat for wireless energy harvesting, the dielectric tissues of the head not only affects the antenna performance, but also the antenna may have harmful effects on the rat head due to RF radiation. Therefore, the interaction of the antenna of the head-mountable DBS device with a rat model needs to be evaluated. The existence of dielectric materials near the antenna influences its performance including the change of input impedance, resonance frequency, radiation efficiency, and radiation pattern [8]. Moreover, the incident EM wave from the far field energy transmitter, and the electrical current in the receiving antenna generated by the harvested energy induce an EM field in surrounding head or body tissues. The induced EM field can harm biological tissues by destroying molecular structure, and rising tissue temperature [9]. Hence, the biological compatibility analysis owing to the EM absorption in rat body tissue is another crucial issue. Therefore, challenges for an energy harvesting antenna in a head-mountable DBS device are: (i) design of a small and high performing receiving antenna, (ii) analysis of the detuning and performance degradation of the antenna with a rat head, and (iii) understanding of the EM field distribution inside the rat body for safety concerns.

II. Antenna Design

A. Antenna Configuration

Fig. 1 illustrates the configuration of the proposed circular meander dipole antenna. The antenna dimension is optimized using EM simulation software by an iterative method. The volume of the design antenna is $\pi \times 14^2 \times 1.6$ mm^3. The radiating metallic patch is printed on a 1.58222 mm thick dielectric substrate *FR-4* of $\varepsilon_r = 4.5$ and $\delta = 0.02$. The copper is used as the fundamental conducting material for this design. The meandering process is applied in both

M. K. Hosain is with the School of Engineering, Deakin University, Victoria, Australia (e-mail: mhosain@deakin.edu.au).

A. Z. Kouzani is with the School of Engineering, Deakin University, Waurn Ponds, Victoria 3216, Australia (e-mail: kouzani@deakin.edu.au).

S. J. Tye is with Department of Psychiatry and Psychology, Mayo Clinic, Rochester MN 55905, USA.

O. A. Abulseoud is with Department of Psychiatry and Psychology, Mayo Clinic, Rochester MN 55905, USA.

M. Berk is with School of Medicine, Deakin University, Waurn Ponds, Victoria 3216, Australia.

radiating poles to increase the length of the current flow path and minimize the overall size of the antenna [2, 10]. The two poles of the antenna are symmetrical, and the direction of current flow is opposite in the two poles. Five meanders are used in each pole of the dipole antenna. The width of each meander is 1.0 mm and the width of the metal between the two meanders is also 1mm. The length of the conventional dipole antenna is about half of the resonant wavelength which is 163 mm at 915 MHz. Since in this design each arms of the dipole are meandered, the size of the antenna is considerably reduced compared to the conventional dipole, L-shape dipole [11], and G-shape dipole [12] antennas.

A 50 Ω feed line is used as a requirement of the software to supply input to the radiating patch. The impedance of the feed line did not match with the input impedance of the antenna because the typical input impedance of a half wave dipole is about 73 Ω. To match the feed line impedance with the antenna input impedance, a single stub matching technique is employed and integrated with the antenna. It should be pointed out that the shorting stub is used to adjust the inductive reactance which minimizes the capacitive coupling between the two arms of the dipole [13]. The length and position of the stub is varied iteratively to achieve a good impedance match. The complete antenna structure with suitable matching element is shown in Fig. 1. Nevertheless, the designed antenna is suitable for head-mountable DBS devices due to its small size and round structure.

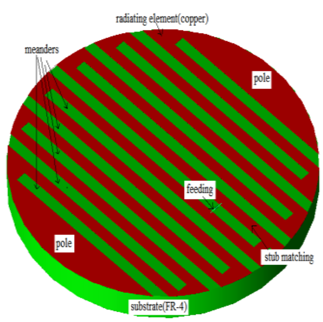

Fig. 1 Configuration of the proposed dipole antenna.

B. *Antenna Performance in Free Space*

An iterative simulation test using EM simulation software XFdtd is done to get the optimal antenna parameters including return loss and gain pattern. Fig. 2 shows the frequency response of the return loss (S_{11}) of the proposed dipole antenna. The resonant frequency of the designed dipole antenna is 915 MHz which is at the ISM band. The ISM band of 915 MHz is a good candidate for this research because of the frequency is higher than the MICS band of 402 MHz, thus offering small antenna size and high data rate. Moreover, the frequency of 915 MHz is lower than the ISM band of 2.4 GHz, therefore providing less dielectric loss inside biological tissues. The input impedance of the designed antenna is Z_i = 47.25 − 2.918j at 915 MHz. The antenna is capacitive at operating frequency of 915 MHz. The bandwidth of 15 MHz (905 – 920 MHz) at a return loss of -10 dB is attained in this design. Fig. 3 shows the simulated far field gain pattern of the designed antenna at $\phi = 0^o$ and $\phi = 90^o$. Apparently, the gain pattern at $\phi = 0^o$ is similar to omnidirectional and the pattern at $\phi = 90^o$ is dipole-like which are analogous to the conventional dipole antenna characteristics. The maximum gain value of −4.1 dB is recorded at $\phi = 0^o$ and $\theta = 90^o$. The radiation efficiency of the proposed antenna is 14.61% at free space. Since it is intended to use the proposed antenna with a head-mountable DBS device for laboratory rat studies, the antenna parameters are changed due to the rat body interaction. The consequences of the interaction of the rat model with the dipole antenna are described in Section III.

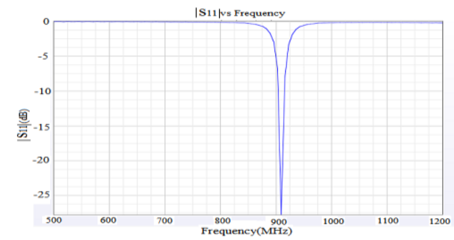

Fig. 2 Simulated S11 of the antenna in free space.

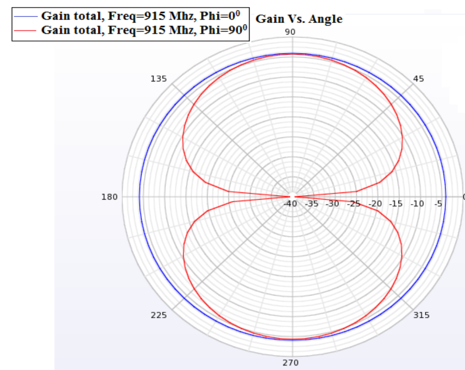

Fig. 3 2D gain pattern of the antenna in free space.

III. Interaction of the Antenna with a Rat Model

The investigation of the interaction of the rat body with the designed antenna for the head-mountable DBS device can be classified as: functional and biological. The functional aspect analyses the change of the antenna parameters including refection coefficient, efficiency, and radiation pattern due to the loading effects by the rat body. On the other hand, the biological aspect examines the impact of the antenna on the rat model in terms of EM field distribution, and SAR value [8]. The evaluation of the characteristics of the dipole antenna in the vicinity of the rat model needs to be specified to establish a reliable energy harvesting link. The biological compatibility analysis is essential for safety regulation, and identification of stimulating signal effects on the rat in DBS research.

A. *Functional Aspect*

The antenna performance parameters including input impedance, resonance frequency, gain pattern, and efficiency are simulated with a complete rat model because the antenna needs to be used in a head-mountable DBS device. A complete rat model used in this simulation consists of a complete rat body with thirteen different dielectrics tissues. This rat model is collected from Remcom XFdtd EM simulation software supporting center, and used with the XFdtd software library in the simulation. The dielectric properties of the materials used in the rat model at 915 MHz are shown in Table I. The configuration of the complete rat model including the circular meander dipole antenna is shown in Fig. 4. The antenna is simulated while mounted on the complete rat model.

The antenna input impedance was altered and the resonance frequency was shifted due to the influence of the nearby rat body tissue. The resonance frequency of the dipole antenna with the rat model was shifted towards lower frequencies. The resonance frequency shift was 125 MHz compared with the free space resonance frequency. These changes of resonance frequency and input impedance are mitigated by reducing the length of the meanders, and by varying the length of the stub correspondingly. After adjusting the length of meanders and feeding position, the simulated S-parameter and input impedance of −22.7 dB and 56.79−4.46j Ω are noted, respectively. The voltage standing wave ratio of the simulated antenna with the complete rat model is 1.165. The far field gain pattern of the designed antenna with the complete rat model is represented in Fig. 5. The maximum value of the antenna gain is −12.18 dB at $\phi = 0^o$ and $\theta = 270^o$. The radiation pattern found with rat model is different than that in free space. The change of shape of the radiation pattern is due to the loading effects of the rat model at the ISM band. The antenna radiation efficiency with the rat model is 3.17 % which is lower than the free space radiation efficiency due to the losses in the rat model.

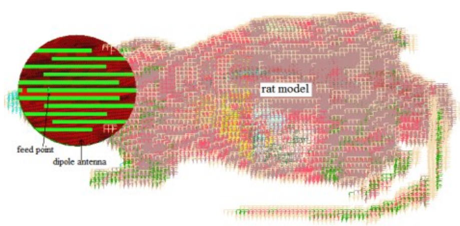

Fig. 4 Complete rat model and the dipole antenna.

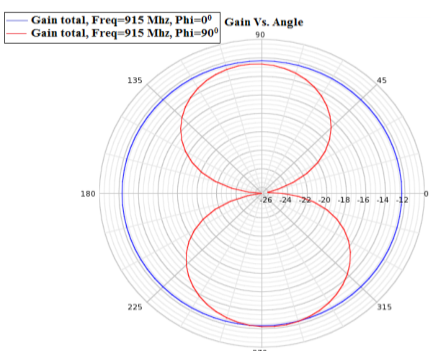

Fig. 5 2D far field gain pattern with the complete rat model.

B. Biological Aspect

SAR is the biocompatibility analysis factor used to evaluate the ultra-high frequency radiation effects on rat body to determine the safety level. The proposed dipole antenna receives the far field RF EM energy wirelessly while operating on-board of a passive head-mountable DBS device. A part of the incident EM fields from the far field energy transmitter interacts with the biological tissue surrounding the receiving antenna. Moreover, the current flow in the receiving antenna due to the induced energy generates EM field around it. In order to assess the amount of EM power absorbed by the surrounding tissues consequently measuring biocompatibility, a numerical analysis of the SAR is performed at 915 MHz for the simulation setup that is shown in Fig. 4. In this simulation setup, the proposed dipole antenna is assumed to feed by a source with equivalent received power.

A simulation of our designed antenna is performed with a complete rat model as the proposed device is assumed to use with laboratory rat study. Since the electric field and magnetic field distribution are similar and SAR is directly related to electric field value, electric field distribution and the evaluation of average SAR are performed in this study. The electric field value in the rat model depends on the duration of the incident wave. The value of the electric field in the rat body increases with the duration of the operating time of the device.

Fig. 6 illustrates the steady state electric field in the planes of the patch antenna where 1-g and 10-g average SAR is maximum. The CAD display of the rat body and antenna is turned off to view the internal fields. The antenna received power is scaled to 1 W in this simulation. The value of the maximum electric field in slices of 1-g and 10-g average SAR are 698.03 V/m, and 4399.8 V/m, respectively. The deposition and penetration of electric field values depends on the dielectric properties of the rat model. The electric field which penetrates the bone of the head and reaches in deeper position of the brain tissues is higher than the standard regulated value as in [17] because of the antenna's received power of 1 W. It is obvious that the electric field distribution will be within the standard regulated limit if the antenna's received power reaches to a few mW range.

TABLE I. DIELECTRIC PROPERTIES OF THE RAT MODEL AT 915MHZ [14-16].

Layer Name	Relative Permittivity	Conductivity (s/m)	Mass Density (kg/m^3)
Skin etc	41.2	0.9	1109
Fat etc	11.37	0.11	978
Bone	4.9	0.15	1180
Body fluid etc	67.5	1.75	1019
aorta	42	0.776	1040
Gray matter etc	50	1.0	1041
Nerve etc	37.6	0.684	1085
Tooths etc	12.4	0.145	1730
Muscle etc	55	0.948	1045
Liver etc	46	1.06	1037
Blood etc	61.38	1.56	1050
bladder	20.5	0.32	1030
Inner lung	33	0.78	260

The analysis of SAR can give us more insight of the EM power absorption inside the rat body tissue. The calculation method of SAR depends on the distribution of the electric field. Fig. 7 shows the slices of 1 g average and 10-g average SAR values in the plane of the patch antenna where SAR is maximum. The CAD display of the body tissues and antenna is switched off to view the internal result. The maximum 1g average SAR value of 129.59 W/kg, and 10-g average SAR value of 28.56 W/kg are recorded in this simulation which are higher than the standard IEEE C95.1-1999 (1-g average SAR<1.6 W/kg) [18], and IEEE C95.1-2005 (10-g average SAR<2 W/kg) [19]. The average SAR over the complete rat model is 4.54 W/kg. To maintain the safety regulation for 1g average SAR imposed by American National Standards Institute regulation [18], the received/delivered power by our proposed antenna should be less than 12.35 mW.

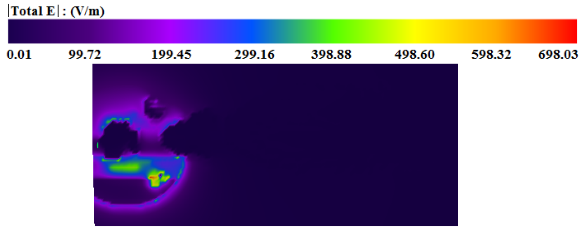

(a)

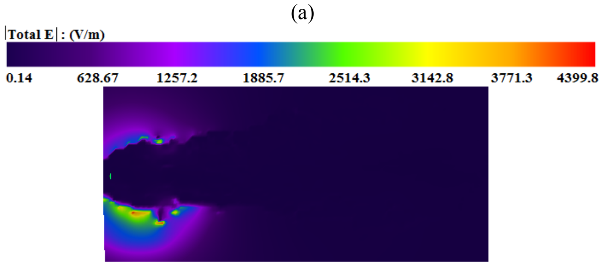

(b)

Fig. 6 Electric field distribution in the plane of the patch antenna at the slice of maximum value of 1-g average SAR (a), and 10-g average SAR (b).

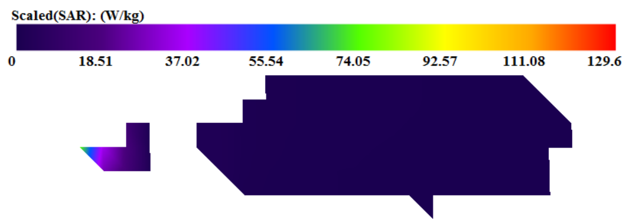

(a)

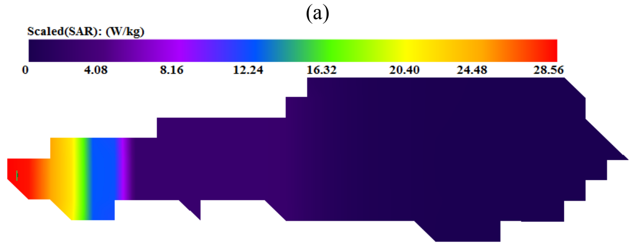

(b)

Fig. 7 (a) 1-g SAR values in the plane of the patch antenna at the slice of maximum value. (b) 10-g SAR values in the plane of the patch antenna at the slice of maximum value.

IV. Conclusion

This paper presented a circular meander dipole antenna, for a head-mountable passive DBS device. Moreover, the paper investigated the interaction of the antenna with a rat model in functional and biological aspects. The designed antenna had the bandwidth of 15 MHz (905 – 920 MHz) at a return loss of -10 dB at ISM band of 915 MHz, and the maximum antenna gain of −4.1 dB at free space. The existence of rat model near the proposed antenna has altered the antenna parameters. The shift of resonance frequency was 125 MHz, and the reduction of antenna gain was 8.08 dB with the complete rat model. The SAR penetration and deposition depend on the dielectric properties of biological tissues and the separation between antenna and tissues. The EM field, and average SAR values in rat model generated by the receiving antenna, assuming that the receiving power of 1 W, were higher than the standard regulated value. To maintain the safety regulation imposed by IEEE C95.1-1999 standard, the received power of the proposed dipole antenna for power harvesting to a passive head-mountable DBS device should be less than few mWs. Since it is simulation based study, a comprehensive experimental evaluation is required before concluding about the performance and safety regulation of this proposed device.

References

[1] H. Jabbar, Y. S. Song, and T. T. Jeong, "RF energy harvesting system and circuits for charging of mobile devices," Consumer Electronics, IEEE Transactions on, vol. 56, pp. 247-253, 2010.

[2] M. K. Hosain, A. Z. Kouzani, S. Tye, and D. Mortazavi, "Compact stacked planar inverted-F antenna for passive deep brain stimulation implants," in Engineering in Medicine and Biology Society (EMBC), 2012 Annual International Conference of the IEEE, 2012, pp. 851-854.

[3] B. Jiang, J. R. Smith, M. Philipose, S. Roy, K. Sundara-Rajan, and A. V. Mamishev, "Energy scavenging for inductively coupled passive RFID systems," in Instrumentation and Measurement Technology Conference, 2005. IMTC 2005. Proceedings of the IEEE, 2005, pp. 984-989.

[4] A. Harb, "Energy harvesting: State-of-the-art," Renewable Energy, vol. 36, pp. 2641-2654, 2011.

[5] J. A. Paradiso and T. Starner, "Energy scavenging for mobile and wireless electronics," Pervasive Computing, IEEE, vol. 4, pp. 18-27, 2005.

[6] Y. Hu, M. Sawan, and M. N. El-Gamal, "An integrated power recovery module dedicated to implantable electronic devices," Analog Integrated Circuits and Signal Processing, vol. 43, pp. 171-181, 2005.

[7] E. M. Yeatman, "Advances in power sources for wireless sensor nodes," in Proc. Int'l Workshop Wearable and Implantable Body Sensor Networks, 2004, pp. 20-21.

[8] A. Andújar, J. Anguera, C. Picher, and C. Puente, "Human Head Interaction Over Ground Plane Booster Antenna Technology: Functional and Biological Analysis," Progress In Electromagnetics Research B, vol. 41, pp. 153-185, 2012.

[9] A. Lak, "Human Health Effects from Radiofrequency and Microwave Fields," Journal of Basic and Applied Scientific Research, vol. 2, pp. 12302-05, 2012.

[10] K.-L. Wong, Compact and broadband microstrip antennas. New York: John Wiley & Sons, Inc., 2002.

[11] S. W. Su and J. H. Chou, "Compact coaxial- line- fed flat- plate dipole antenna for WLAN applications," Microwave and Optical Technology Letters, vol. 50, pp. 420-422, 2008.

[12] X. Li, L. Yang, S. X. Gong, Y. J. Yang, and J. F. Liu, "A compact folded printed dipole antenna for UHF RFID reader," Progress In Electromagnetics Research Letters, vol. 6, pp. 47-54, 2009.

[13] S. W. Su and J. H. Chou, "Low-cost flat metal-plate dipole antenna for 2.4/5-GHz WLAN operation," Microwave and Optical Technology Letters, vol. 50, pp. 1686-1687, 2008.

[14] C. Gabriel, S. Gabriel, and E. Corthout, "The dielectric properties of biological tissues: I. Literature survey," Phys. Med. Biol., vol. 41, p. 2231, 1999.

[15] R. Pethig, "Dielectric properties of body tissues," Clin. Phys. Physiol. Meas., vol. 8, pp. 5-12, 1987.

[16] S. Bri, S. Kassimi, M. Habibi, and A. Mamouni, "Specific absorption rate (SAR) distribution in the human head at global system mobile (GSM) frequencies," European J. Sci. Res., vol. 49, pp. 590-600, 2011.

[17] A. Ahlbom, U. Bergqvist, J. Bernhardt, J. Cesarini, M. Grandolfo, M. Hietanen, A. Mckinlay, M. Repacholi, D. Sliney, and J. Stolwijk, "Guidelines for limiting exposure to time-varying electric, magnetic, and electromagnetic fields (up to 300 GHz). International Commission on Non-Ionizing Radiation Protection," Health Phys, vol. 74, pp. 494-522, 1998.

[18] S. Gabriel, R. Lau, and C. Gabriel, "The dielectric properties of biological tissues: II. Measurements in the frequency range 10 Hz to 20 GHz," Physics in medicine and biology, vol. 41, p. 2251, 1999.

[19] "IEEE Standard for Safety Levels With Respect to Human Exposure to Radio Frequency Electromagnetic Fields, 3 kHz to 300 GHz," IEEE Std C95.1-2005 (Revision of IEEE Std C95.1-1991), pp. 0_1-238, 2006.